



HAL
open science

Path Optimization for Humanoid Walk Planning: an Efficient Approach

Antonio El Khoury, Michel Taïx, Florent Lamiraux

► **To cite this version:**

Antonio El Khoury, Michel Taïx, Florent Lamiraux. Path Optimization for Humanoid Walk Planning: an Efficient Approach. Proceedings of the 8th International Conference on Informatics in Control, Automation and Robotics, Jul 2011, Noordwijkerhout, Netherlands. pp.179 - 184. hal-00572375v3

HAL Id: hal-00572375

<https://hal.science/hal-00572375v3>

Submitted on 21 Jun 2011

HAL is a multi-disciplinary open access archive for the deposit and dissemination of scientific research documents, whether they are published or not. The documents may come from teaching and research institutions in France or abroad, or from public or private research centers.

L'archive ouverte pluridisciplinaire **HAL**, est destinée au dépôt et à la diffusion de documents scientifiques de niveau recherche, publiés ou non, émanant des établissements d'enseignement et de recherche français ou étrangers, des laboratoires publics ou privés.

PATH OPTIMIZATION FOR HUMANOID WALK PLANNING: AN EFFICIENT APPROACH

Antonio El Khoury^{1,2}, Michel Taïx^{1,2}, Florent Lamiraux^{1,2}

¹CNRS ; LAAS ; 7 avenue du colonel Roche, F-31077 Toulouse Cedex 4, France

²Université de Toulouse ; UPS, INSA, INP, ISAE ; UT1, UTM, LAAS ; F-31077 Toulouse Cedex 4, France
aelkhour@laas.fr; taix@laas.fr; florent@laas.fr

Keywords: humanoid robot, motion planning, walk planning, holonomic constraints, optimization, A*, HRP-2.

Abstract: This paper deals with humanoid walk planning in cluttered environments. It presents a heuristic and efficient optimization method that takes as input a path computed for the robot bounding box, and produces a path where a discrete set of configurations is reoriented using an A* search algorithm. The resulting trajectory is realistic and time-optimal. This method is validated in various scenarios on the humanoid robot HRP-2.

1 RELATED WORK AND CONTRIBUTION

The problem of humanoid walk planning can be defined as follows: given an environment and a humanoid robot with start and goal placements, a collision-free trajectory needs to be found. It should ideally represent realistic human motion, i.e. a motion similar to that of a human being in the same conditions. This result is desirable since humanoid robots are bound to move in man-made environments such as homes, offices, and factories and because it can help them blend in among humans.

1.1 Humanoid Walk Planning

The problem of motion planning is now well formalized in robotics and several books present the various approaches (Latombe, 1991; Choset et al., 2005; LaValle, 2006). Sampling-based methods rely on random sampling in the configuration space (CS) and use for instance Probabilistic Roadmaps (PRM) (Kavraki et al., 1996) or Rapidly-Expanding Random Trees (RRT) (Kuffner and LaValle, 2000). With these methods it is possible to solve problems for systems with large numbers of Degrees of Freedom (DoF).

The motion planning problem is certainly a complex one in the case of humanoid robots, which are high-DoF redundant systems that have to verify



Figure 1: Humanoid Robot HRP-2 uses holonomic motion, or side-stepping, to pass between two chairs.

bipedal stability constraints. Various planning strategies can be found in literature.

One category relies on whole-body task planning: kinematic redundancy is used to accomplish tasks with different orders of priorities (Khatib et al., 2004; Kanoun et al., 2009). Static balance and obstacle avoidance can thus be defined as tasks that the algorithm has to respect.

Works of (Kuffner et al., 2001; Chestnutt et al., 2005) describe in particular humanoid footstep planning schemes. Starting from an initial footstep placement, they use an A* graph search (Hart et al., 1968) to explore a discrete set of footstep transitions. The search stops when the neighborhood of the goal foot-

step placement is reached. This approach is not practical in some environments with narrow passages, and (Xia et al., 2009) reduced the computational cost of footstep planning by using an RRT planning algorithm.

Another strategy consists of dividing a high-dimensional problem into smaller problems and solving them successively (Zhang et al., 2009). The idea of dividing the problem into a two-stage scheme is described in (Yoshida et al., 2008): A 36-DoF humanoid robot is reduced to a 3-DoF bounding box. Using the robot simplified model, the PRM algorithm solves the path planning problem and generates a feasible path for the bounding box. A geometric decomposition of the path places footsteps on it, and a walk pattern generator based on (Kajita et al., 2003) finally produces the whole-body trajectory for the robot. In (Moulard et al., 2010), this two-stage approach is also used; numerical optimization of the bounding box path produces a time-optimal trajectory that is constrained by foot speed and distance to obstacles.

Another important issue is the notion of holonomic motion: while wheeled robots always remain tangent to their path, thus following a nonholonomic constraint, legged robots can also move sideways, and their motion can be described as holonomic. The path planning scheme in (Yoshida et al., 2008) is designed to this end; a PRM algorithm first builds a roadmap with Dubins curves (Dubins, 1957); but such curves impose a nonholonomic constraint and narrow passages cannot be crossed. The roadmap is therefore enriched with linear local paths. As a result this planning scheme generates motion such that the robot remains tangent to its path most of the time and uses sidestepping only in narrow passages.

Furthermore, (Mombaur et al., 2010) conducted a series of walking experiments that allowed them to build a model of human walking trajectories; if a human being walks long distances, his body tends to be tangential to his path, while holonomic motion is used over smaller distances. This is an attractive property for computed paths if a realistic motion is to be achieved, and holonomic motion can as well be used to pass through narrow spaces. These results suggests that a good combination of both nonholonomic and holonomic motions can be used to achieve realistic walking.

1.2 Contribution

The work of (Moulard et al., 2010) solves the walk planning problem in a natural way, i.e. it uses numerical optimization to minimize the robot walking along the path while following speed and obstacle distance

constraints. After having tried this approach, it was empirically concluded that achieving successful numerical optimization in any kind of environment is a difficult and computationally expensive task; in fact, it requires computing a large set of parameters to fully define the optimized path.

While using the same two-stage approach of (Yoshida et al., 2008), a simpler heuristic method that generates realistic time-optimal humanoid trajectories is proposed. First the PRM algorithm and the Dubins local paths are replaced with an RRT-Connect algorithm and linear local paths. The path is then optimized by locally reorienting the robot bounding box on a discrete set of configurations of the path. Priority to nonholonomic motion is considered and holonomic motion is used only to pass in narrow passages and to avoid nearby obstacles.

The following section presents this method and explains how it is integrated in the motion planning scheme. Examples of different scenarios, including a real one with the HRP-2 platform, are shown in section 3.

2 OPTIMIZATION BY REGULAR SAMPLING

Assuming full knowledge of the environment, the RRT algorithm produces a collision-free piecewise linear path P_{RRT} for the robot bounding box (in offline mode), i.e. the path consists of the concatenation of

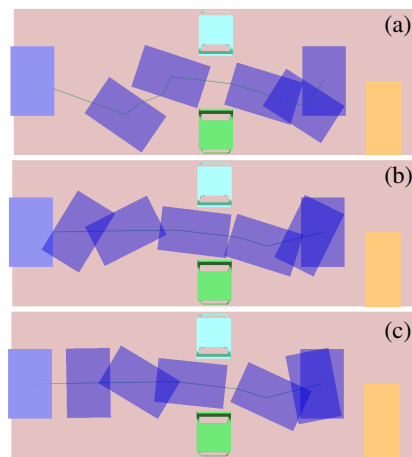


Figure 2: Top view: (a) RRT-Connect path for the bounding box passing between two chairs. (b) Optimized bounding box path by random optimization (RO). (c) Optimized bounding box after adding regular sampling optimization (RSO).

linear local paths LP_{RRT} .

Due to the probabilistic nature of RRTs, P_{RRT} may not be optimal in terms of length, and a preliminary random shortcut optimization (RO) can be run in order to shorten it (See Figure 2). While the optimized path P is collision-free, the bounding box orientation is such that it could lead to an unrealistic trajectory that is not time-optimal. For instance, the humanoid robot could spend a long time walking sideways or backwards over a long distance in an open space. An additional optimization stage is introduced to address this issue in the next section.

2.1 Bounding Box Path Optimization

Note that each configuration q can be written as $q = (\mathbf{X}, \theta)$, where $\mathbf{X} = (x, y)$ describes the bounding box position in the horizontal plane, and θ gives its orientation. The optimizer reorients the bounding box along P by changing θ while retaining the value of \mathbf{X} .

For this purpose, an A* search algorithm is executed; first P is regularly sampled. Using a discrete set of possible orientations for each sample configuration and an adequate heuristic estimation function, the bounding box orientation is then modified along P . An optimized path P_{opt} is created and leads to a realistic time-optimal trajectory.

2.1.1 Preliminary Notations

After running RO on the piecewise linear path P_{RRT} , the path P is also piecewise linear, and its first and last configurations are denoted by q_s and q_g .

Let $d_{sample} \in \mathbb{R}_+^*$ be a sampling distance. Sampling P with a distance d_{sample} means dividing each local path LP_j of P into smaller local paths of length d_{sample} ; each new local path end is a sample configuration. The n^{th} sample configuration of P in its initial state can be obtained by indexing new local path ends starting from q_s , and is denoted by q_n^{init} .

The possible orientation states need to be defined. We aim to make a humanoid robot reach its goal as soon as possible. Since the robot is faster while walking straight than side-stepping, we attempt to change the orientation of each initial sample configuration q_n^{init} such that the bounding box is tangent to the local path and introduce a new configuration denoted by q_n^{front} . To take into account the fact that there may be obstacles that forbid a frontal orientation, we also create $q_n^{lat_1}$ and $q_n^{lat_2}$ that are rotated by $\frac{\pi}{2}$ and $-\frac{\pi}{2}$ relative to the path tangent, see Figure 3. One particular case is local path end configurations: the mean direction of the two adjacent local paths is considered to define frontal and lateral configurations. This is done to

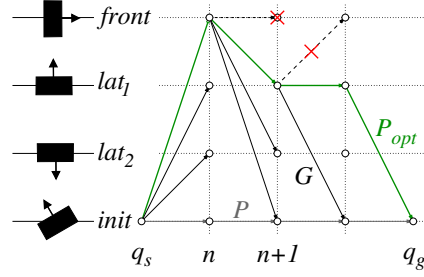


Figure 3: Each initial sample configuration can be rotated and be in one of four states. Starting from q_s , the A* search algorithm searches the graph G that contains only valid nodes and arcs to produce an optimized path P_{opt} .

ensure a smooth transition between two local paths.

A sample configuration whose orientation is unknown will be denoted by q_n^{state} . It can have any orientation state of the set $\{init, front, lat_1, lat_2\}$ except for q_s and q_g which remain in their initial state. Ideally, the algorithm should be able (as long as there are no obstacles) to put each sample configuration in the frontal state, create a new path P_{opt} and generate a time-optimal trajectory for the robot.

An A* search is run to achieve this goal; the algorithm functions are described in the following section.

2.1.2 A* Function Definition

An A* search algorithm can find an optimal path in a graph as long as a graph and an evaluation function are correctly defined. Starting from q_s , A* expands in each iteration the possible transitions from one sample to the next one in the graph and evaluates with the evaluation function the cost of going through each different state, see Figure 3.

A graph G is defined to be a set of nodes and arcs. A valid node $q_n^{state_n}$ is defined to be a configuration with no collisions, and a valid arc $q_n^{state_n} q_{n+1}^{state_{n+1}}$ is a collision-free local path. The whole graph G could be built before running A* by testing all nodes and arcs and making sure they are collision-free. But collision tests are slow, and A* uses a heuristic estimation function to avoid going through all nodes. An empty graph G is thus initialized and nodes and arcs are built only when necessary. A successor operator needs to be defined for this purpose.

The Successor operator $\Gamma(q_n^{state_n})$: Its value for any node $q_n^{state_n}$ is a set $\{(q_{n+1}^{state_{n+1}}, c_{n,n+1})\}$, where $q_{n+1}^{state_{n+1}}$ denotes a successor node, and $c_{n,n+1}$ is the cost of going from $q_n^{state_n}$ to $q_{n+1}^{state_{n+1}}$. The cost $c_{n,n+1}$ is defined to be the distance $D(q_n^{state_n}, q_{n+1}^{state_{n+1}})$ be-

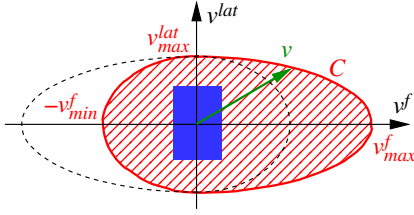


Figure 4: The rectangular bounding box speed vector v is bounded inside the hashed area defined by the speed constraint C . The area is bounded by the union of two half-ellipsoids.

tween two nodes of G ; it computes the walk time from $q_n^{state_n}$ to $q_{n+1}^{state_{n+1}}$. The speed constraint C is defined as:

$$C = \begin{cases} \left(\frac{v^f}{v_{max}^f}\right)^2 + \left(\frac{v^{lat}}{v_{max}^{lat}}\right)^2 - 1 & \text{if } v^f \geq 0 \\ \left(\frac{v^f}{v_{min}^f}\right)^2 + \left(\frac{v^{lat}}{v_{max}^{lat}}\right)^2 - 1 & \text{if } v^f < 0 \end{cases} \quad (1)$$

where v^f and v^{lat} are respectively the frontal and lateral speed, and v_{min}^f , v_{max}^f and v_{max}^{lat} their minimum and maximum values (See Figure 4). $D(q_n^{state_n}, q_{n+1}^{state_{n+1}})$ can be then computed by integrating this speed constraint along it.

Having expressed the successor operator, which allows the optimizer to choose which node to expand at each iteration, the A* evaluation function can be defined.

The Evaluation Function $\hat{f}(q_n^{state})$: It is the estimated cost of an optimal path going through q_n^{state} from q_s to q_g and can be written as:

$$\hat{f}(q_n^{state}) = \hat{g}(q_n^{state}) + \hat{h}(q_n^{state}) \quad (2)$$

where $\hat{g}(q_n^{state})$ is the estimated cost of the optimal path from q_s to q_n^{state} and $\hat{h}(q_n^{state})$ is a heuristic function giving the estimated cost of the optimal path from q_n^{state} to q_g .

$\hat{h}(q_n^{state})$ must verify $\hat{h}(q_n^{state}) \leq h(q_n^{state})$ to ensure that the algorithm is admissible, i.e. the path from q_s to q_g is optimal. Since the robot is fastest while walking straight forward in the absence of obstacles, $\hat{h}(q_n^{state})$ is defined as:

$$\begin{aligned} \hat{h}(q_n^{state}) = & D(q_n^{state}, q_{n+1}^{front}) \\ & + \sum_{k=1}^{N_{sample}-n-2} D(q_{n+k}^{front}, q_{n+k+1}^{front}) \\ & + D(q_{n+1}^{front}, q_g) \end{aligned} \quad (3)$$

where N_{sample} is the total number of initial sample configurations in P including q_s and q_g . $\hat{h}(q_n^{state})$ thus

sums the cost of walking along P while staying tangential to the path with the start and end transition costs from q_n^{state} and to q_g .

Now that the A* functions are fully defined, a search algorithm can be run to compute an optimal path P_{opt} by changing the orientation of each sample node. An example is shown in Figure 5.

2.2 Motion Generation for a Humanoid Robot

A collision-free path P for the 3-DoF bounding box can be found using RRT-Connect and RO. The regular sampling optimization (RSO), which is the subject of this paper, is then applied on the path and produces a path P_{opt} that gives priority to nonholonomic motion.

Once the bounding box trajectory is computed, the robot has to walk along it. A footstep sequence is thus generated along P_{opt} by geometric decomposition of the path, and the pattern generator cited in subsection 1.1 then produces the robot whole-body trajectory.

3 EXAMPLES

This section presents experimental results of the path optimizer after it has been inserted in the previously described walk planning scheme. Distance parameters v_{max}^f , v_{max}^{lat} , v_{min}^f are set to 0.5, 0.1, and 0.25 respectively. d_{sample} is equal to $\frac{h}{6}$, where h is the humanoid's height. Tests are performed on a 2.13 GHz Intel Core 2 Duo PC with 2 GB RAM.

Simulations of the humanoid robot HRP-2 are run in three scenarios. The first one is a small en-

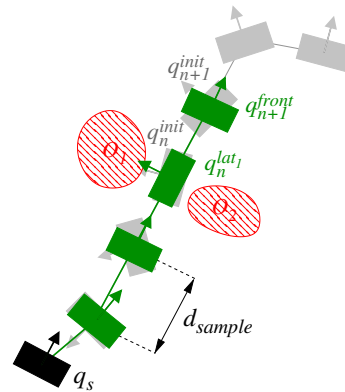


Figure 5: Local paths are regularly sampled (light grey) and each sample configuration is reoriented (dark) while considering obstacles O_1 and O_2 .

Table 1: Columns 1 to 5: Computational time (ms) of each planning stage for the presented scenarios. Columns 6 and 7: Humanoid robot walk time (s) for the presented scenarios using RO alone and a RO-RSO combination.

	RRT-Connect	RO	RSO	Robot Trajectory	Total	RO	RO+RSO
Chairs	3,968	1,887	2,144	66,140	74,140	40	35
Galton	91.69	2,497	237.8	65,730	68,560	66	57
Apartment	1,212	2,425	2,412	222,800	228,800	200	120

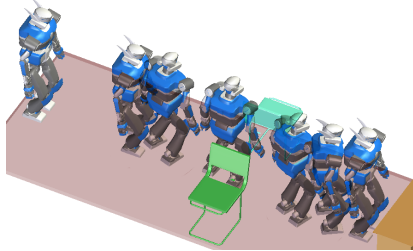


Figure 6: Perspective view of the simulated HRP-2 trajectory on the final optimized path passing between two chairs.

environment where HRP-2 has to pass between two chairs. The second environment is uncluttered with few obstacles lying around, while the last one is a bigger apartment environment where the robot has to move from one room to another while passing through doors. The chairs scenario motion is also replayed on the real robot HRP-2 (See Figure 1). Videos for all scenarios can be viewed at <http://humanoid-walk-planning.blogspot.com/>

Table 1 shows computation times for each stage of the planning scheme: RRT-Connect, RO, RSO, and the whole-body robot trajectory generation. In order to show the optimizer contribution, robot walk times are also measured by creating a trajectory directly after RO, and comparing it with a trajectory where the RSO was added.

3.1 “Chairs” Scenario

Figure 2 shows the bounding box RRT path and the RO path for the chairs scenario. It is obvious that RO creates a shorter path, but the bounding box starts rotating from the beginning of the path even though the two chairs are still far. This causes the robot trajectory to be unrealistic on one hand and, since walking sideways takes a longer time than walking straight, to also not be time-optimal.

However, after applying RSO, it is clear that the bounding box stays oriented towards the front and rotates only when it reaches the chairs. Figure 6 and Table 1 show that the walk time is shorter by 5 s and the final trajectory for HRP-2 is more realistic. Note that the RSO takes 2,144 ms to be executed on the chairs path, which is less than 3% of the total computation

time.

3.2 “Galton” Scenario

An uncluttered environment is considered in this case, and it can be seen that RRT-Connect and RSO computation times are very low compared to other environments. This can be explained by the fact that a tree connecting start and goal configurations is easier to find, and that the frontal orientation state is valid for all considered samples on the path (See Figure 7).

3.3 “Apartment” Scenario

The planning scheme is finally applied in the apartment scenario. In Figure 8, it is evident that HRP-2 walks facing forward through the doors. As with previous scenarios, the trajectory is more realistic than a trajectory where RSO is not used. The added computation time for RSO is 2,412 ms, which is insignificant compared to the 228 s it takes for the whole planning scheme.

Additionally, since the environment is significantly larger and more constrained than the previous ones, the walk time difference is more striking: Table 1 shows that it takes the robot 80 s less to cross the apartment when an RO-RSO combination is used.

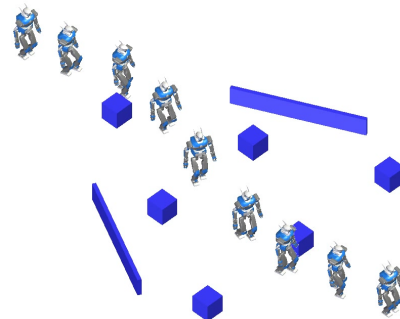


Figure 7: Perspective view of HRP-2 optimized trajectory in the Galton board scenario.

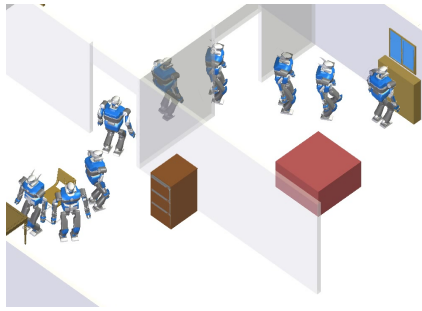


Figure 8: Perspective view of HRP-2 optimized trajectory in the apartment scenario.

4 CONCLUSION

In this paper, a novel simple optimization method is presented for humanoid walk planning that relies on a decoupling between trajectory and robot orientations. It uses an A* search that takes as input a path for the robot bounding box, and produces a path where a discrete set of configurations have been reoriented to generate a realistic time-optimal walk trajectory. Results show that new trajectories are more satisfactory while the added computation time is insignificant compared to the whole planning time.

Of course, this approach can be used in other fields such as graphical animation for digital actors to adapt the body orientation with respect to the goal during locomotion. With a motion capture library containing pre-recorded nonholonomic and holonomic walk behaviors, it is possible to lay this behavior on the actor trajectory and produce realistic movements.

ACKNOWLEDGEMENTS

This work was supported by the French FUI Project ROMEO.

REFERENCES

Chestnutt, J., Lau, M., Cheung, G., Kuffner, J., Hodgins, J., and Kanade, T. (2005). Footstep planning for the honda asimo humanoid. In *Robotics and Automation, 2005. ICRA 2005. Proceedings of the 2005 IEEE International Conference on*, pages 629 – 634.

Choset, H., Lynch, K. M., Hutchinson, S., Kantor, G. A., Burgard, W., Kavraki, L. E., and Thrun, S. (2005). *Principles of Robot Motion: Theory, Algorithms, and Implementations*. MIT Press, Cambridge, MA.

Dubins, L. E. (1957). On curves of minimal length with a constraint on average curvature, and with prescribed

initial and terminal positions and tangents. *American Journal of Mathematics*, 79(3):pp. 497–516.

Hart, P., Nilsson, N., and Raphael, B. (1968). A Formal Basis for the Heuristic Determination of Minimum Cost Paths. *IEEE Transactions on Systems Science and Cybernetics*, 4(2):100–107.

Kajita, S., Kanehiro, F., Kaneko, K., Fujiwara, K., Harada, K., Yokoi, K., and Hirukawa, H. (2003). Biped walking pattern generation by using preview control of zero-moment point. In *Robotics and Automation, 2003. Proceedings. ICRA '03. IEEE International Conference on*, volume 2.

Kanoun, O., Lamiroux, F., Wieber, P.-B., Kanehiro, F., Yoshida, E., and Laumond, J.-P. (2009). Prioritizing linear equality and inequality systems: Application to local motion planning for redundant robots. In *Robotics and Automation, 2009. ICRA '09. IEEE International Conference on*, pages 2939 –2944.

Kavraki, L., Svestka, P., Latombe, J.-C., and Overmars, M. (1996). Probabilistic roadmaps for path planning in high-dimensional configuration spaces. *Robotics and Automation, IEEE Transactions on*, 12(4):566 –580.

Khatib, O., Sentis, L., Park, J., and Warren, J. (2004). Whole-body dynamic behavior and control of human-like robots. *Int. J. Humanoid Robotics*, 1(1):29–43.

Kuffner, J.J., J. and LaValle, S. (2000). Rrt-connect: An efficient approach to single-query path planning. In *Robotics and Automation, 2000. Proceedings. ICRA '00. IEEE International Conference on*.

Kuffner, J.J., J., Nishiwaki, K., Kagami, S., Inaba, M., and Inoue, H. (2001). Footstep planning among obstacles for biped robots. In *Intelligent Robots and Systems, 2001. Proceedings. 2001 IEEE/RSJ International Conference on*.

Latombe, J.-C. (1991). *Robot Motion Planning*. Kluwer Academic Publishers, Norwell, MA, USA.

LaValle, S. M. (2006). *Planning Algorithms*. Cambridge University Press, Cambridge, U.K.

Mombaur, K., Truong, A., and Laumond, J.-P. (2010). From human to humanoid locomotion—an inverse optimal control approach. *Auton. Robots*, 28:369–383.

Moulard, T., Lamiroux, F., and Wieber, P.-B. (2010). Collision-free walk planning for humanoid robots using numerical optimization. Retrieved from <http://hal.archives-ouvertes.fr/hal-00486997/en/>.

Xia, Z., Chen, G., Xiong, J., Zhao, Q., and Chen, K. (2009). A random sampling-based approach to goal-directed footstep planning for humanoid robots. In *Advanced Intelligent Mechatronics, 2009. AIM 2009. IEEE/ASME International Conference on*.

Yoshida, E., Esteves, C., Belousov, I., Laumond, J.-P., Sakaguchi, T., and Yokoi, K. (2008). Planning 3-d collision-free dynamic robotic motion through iterative reshaping. *Robotics, IEEE Transactions on*, 24(5):1186 –1198.

Zhang, L., Pan, J., and Manocha, D. (2009). Motion planning of human-like robots using constrained coordination. In *Humanoid Robots, 2009. Humanoids 2009. 9th IEEE-RAS International Conference on*.